

Tunable metal-insulator transition in $LaTiO_3/CaVO_3$ superlattices: A theoretical study

Ya-Kui Weng(翁亚奎)[1,†], Meng-Lan Shen(沈梦兰)[2], Jie Li(李杰)[3], and Xing-Ao Li(李兴鳌)[1,†]

Citation: Chin. Phys. B, 2020, 29 (**12**): 127303. DOI: 10.1088/1674-1056/abc237
Journal homepage: http://cpb.iphy.ac.cn; http://iopscience.iop.org/cpb

What follows is a list of articles you may be interested in

Single-electron transport through single and coupling dopant atoms in silicon junctionless nanowire transistor

Xiao-Di Zhang(张晓迪), Wei-Hua Han(韩伟华), Wen Liu(刘雯), Xiao-Song Zhao(赵晓松), Yang-Yan Guo(郭仰岩), Chong Yang(杨冲), Jun-Dong Chen(陈俊东), Fu-Hua Yang(杨富华)
Chin. Phys. B, 2019, 28 (**12**): 127302. DOI: 10.1088/1674-1056/ab527a

Observation of hopping transitions for delocalized electrons by temperature-dependent conductance in siliconjunctionless nanowire transistors

Yang-Yan Guo(郭仰岩), Wei-Hua Han(韩伟华), Xiao-Song Zhao(赵晓松), Ya-Mei Dou(窦亚梅), Xiao-Di Zhang(张晓迪), Xin-Yu Wu(吴歆宇), Fu-Hua Yang(杨富华)
Chin. Phys. B, 2019, 28 (**10**): 107303. DOI: 10.1088/1674-1056/ab3e68

Optical response of an inverted InAs/GaSb quantum well in an in-plane magnetic field

Xiaoguang Wu(吴晓光)
Chin. Phys. B, 2019, 28 (**10**): 107302. DOI: 10.1088/1674-1056/ab3c29

Disorder effects in topological states: Brief review of the recent developments

Binglan Wu(吴冰兰), Juntao Song(宋俊涛), Jiaojiao Zhou(周娇娇), Hua Jiang(江华)
Chin. Phys. B, 2016, 25 (**11**): 117311. DOI: 10.1088/1674-1056/25/11/117311

Modulation of physical properties of oxide thin films by multiple fields

Hua-Li Yang(杨华礼), Bao-Min Wang(王保敏), Xiao-Jian Zhu(朱小健), Jie Shang(尚杰), Bin Chen(陈斌), Run-Wei Li(李润伟)
Chin. Phys. B, 2016, 25 (**6**): 067303. DOI: 10.1088/1674-1056/25/6/067303

Tunable metal–insulator transition in $LaTiO_3/CaVO_3$ superlattices: A theoretical study*

Ya-Kui Weng(翁亚奎)[1,†], Meng-Lan Shen(沈梦兰)[2], Jie Li(李杰)[3], and Xing-Ao Li(李兴鳌)[1,‡]

[1] School of Science, Nanjing University of Posts and Telecommunications, Nanjing 210023, China
[2] School of Materials Science and Engineering, Nanjing University of Posts and Telecommunications, Nanjing 210023, China
[3] Grünberg Research Center, Nanjing University of Posts and Telecommunications, Nanjing 210023, China

(Received 14 May 2020; revised manuscript received 12 October 2020; accepted manuscript online 17 October 2020)

As one of intriguing physical results of electronic reconstruction, the metal–insulator transition plays an important role in exploring new electronic devices. In this study, the density functional theory is employed to investigate the metal–insulator transition in $(LaTiO_3)_m/(CaVO_3)_n$ superlattices. Herein, three kinds of physical avenues, *i.e.*, stacking orientation, epitaxial strain, and thickness periods, are used to tune the metal–insulator transition. Our calculations find that the [001]- and [110]-oriented $(LaTiO_3)_1/(CaVO_3)_1$ superlattices on $SrTiO_3$ substrate are insulating, while [111]-oriented case is metallic. Such metallic behavior in [111] orientation can also be modulated by epitaxial strain. Besides the structural orientation and strain effect, the highly probable metal–insulator transition is presented in $(LaTiO_3)_m/(CaVO_3)_n$ superlattices with increasing thickness. In addition, several interesting physical phenomena have also been revealed, such as selective charge transfer, charge ordering, and orbital ordering.

Keywords: metal–insulator transition, superlattices, charge transfer

PACS: 73.21.Cd, 71.30.+h, 73.20.At **DOI:** 10.1088/1674-1056/abc237

1. Introduction

Due to a broad range of novel physical properties in condensed matter physics and material science, perovskite oxides ABO_3 have been intensively investigated as a platform to explore new electronic devices and technical applications.[1–4] With tuning of a control parameter such as composition, temperature, pressure, and epitaxial strain, desirable functional behavior can be obtained.[5–12] In particular, as an intriguing physical phenomena for applications to high-performance switching devices, the metal–insulator transition (MIT) has attracted great interest.[13–15] For example, MIT has been studied by applying the field-effect technique and hole doping of the valence band.[16–18] In addition, a coupled magnetic-ferroelectric MIT with large mixed magnetic–electric–elastic responses was induced by epitaxial train[19]

In recent years, the latest thin film technology in the synthesis of oxides has broadened exciting avenues for the device design and will probably lead the revolution of electronic devices.[20–23] Thus, besides aforementioned physical methods, transition metal–oxide superlattices provide a wider range of strategies to tune MIT. For example, the metal–insulator transition has been observed in $(LaMnO_3)_{2n}/(SrMnO_3)_n$ superlattices with increasing n,[24–27] such thickness-dependent MIT also occurred at the interface between $LaAlO_3$ and $SrTiO_3$.[28] In addition, an effective way to tune MIT in $CaZrO_3/SrTiO_3$ via ionic liquid electrolyte gating has been reported.[29] However, in many previously studied materials, the exploration of MIT for each material is generally limited to one research method. Thus, it would be interesting to use different methods to tune MIT in specific materials.

In this work, $LaTiO_3$ and $CaVO_3$ materials are selected to construct the superlattice, *i.e.*, $LaTiO_3/CaVO_3$ superlattice. There are several physical considerations to discuss. First, both materials have only one d electron, *i.e.*, d^1 configuration, which allows us to observe the changes of electronic structures directly. Second, the identical crystalline structures (orthorhombic No. 62 *Pbnm*) and approximate lattice constants of parent materials ensure the possibility for epitaxial growth of $LaTiO_3/CaVO_3$ superlattices in experiment. Last but not least, considering charge transfer between Ti^{3+} and V^{3+}, it is also interesting to explore whether there is charge transfer between Ti^{3+} and V^{4+}. Here, three kinds of physical avenues, *i.e.*, stacking orientation, epitaxial strain, and thickness periods, are employed to tune the MIT. In the following study, the MIT has been well modulated based on these physical methods. Meanwhile, some interesting physical phenomena, such as charge ordering and orbital ordering, have also been revealed.

*Project supported by the National Natural Science Foundation of China (Grant Nos. 11804168 and 51872145), the Natural Science Foundation of Jiangsu Province, China (Grant Nos. BK20180736 and BK20190726), the Natural Science Foundation of the Jiangsu Higher Education Institutions of China (Grant No. 18KJB140009), and the Science Foundation from Nanjing University of Posts and Telecommunications, China (Grant No. NY219026).

†Corresponding author. E-mail: wyk@njupt.edu.cn
‡Corresponding author. E-mail: lixa@njupt.edu.cn

© 2020 Chinese Physical Society and IOP Publishing Ltd

2. Models and methods

The ground state of bulk $LaTiO_3$ (LTO) is a G-type antiferromagnetic (G-AFM) Mott insulator,[30] while bulk $CaVO_3$ (CVO) is a paramagnetic (PM) metal.[31] The experimental lattice constants (a, b, c) is (5.637, 5.619, 7.916) for LTO[32] and (5.322, 5.343, 7.547) for CVO[33] in units of Å. To address the biaxial strain effects, the widely used cubic $SrTiO_3$ (STO) and $LaAlO_3$ (LAO) are chosen as the substrates, namely, the in-plane lattice constants are fixed to match the particular substrates. To investigate the effects of thickness periods, $(LTO)_1/(CVO)_2$ and $(LTO)_2/(CVO)_2$ superlattices stacked along the [001] orientation are studied, using STO as the substrate.

All the following calculations are performed based on the generalized gradient approximation (GGA) with revised Perdew–Burke–Ernzerhof (PBEsol) potentials,[34] as implemented in the Vienna *ab initio* Simulation Package (VASP).[35,36] The cutoff energy of the plane wave is 520 eV and the on-site Hubbard repulsion U_{eff} ($= U - J$) is imposed on Ti's/V's 3d and La's 4f orbitals using the Dudarev implementation.[37] According to previous literature,[38,39] $U_{\text{eff}}(\text{Ti}) = 3$ eV, $U_{\text{eff}}(\text{V}) = 3$ eV, and $U_{\text{eff}}(\text{La}) = 8$ eV are adopted as default parameters in the following calculations. In our calculations, the relaxed lattice constants are very close to the experimental values,[32,33] and the magnetic moments of bulk LTO is $\sim 0.68\ \mu_B$/Ti. The atomic projected density of states (PDOS) of bulk LTO and CVO are displayed in Figs. 1(d) and 1(e). The states around the Fermi level mainly come from Ti's or V's 3d orbitals. All these results guarantee the reliability of following calculations on superlattices. Monkhorst–Pack k-point meshes of $7 \times 7 \times 5$, $7 \times 5 \times 7$, and $7 \times 7 \times 3$ centered at Γ point are adopted for $(LTO)_1/(CVO)_1$ superlattices stacking along the [001], [110], and [111] orientations respectively, while $5 \times 5 \times 1$ and $3 \times 3 \times 1$ meshes are used for the [001]-orientated $(LTO)_1/(CVO)_2$ and $(LTO)_2/(CVO)_2$ superlattices respectively. Both the out-of-plane lattice constants and atomic positions are fully relaxed until the Hellman–Feynman forces are converged to less than 0.01 eV/Å.

3. Results and discussion

3.1. Stacking orientation

To study the effects of stacking orientation on MIT, three orientations of $(LTO)_1/(CVO)_1$ superlattice, *i.e.*, [001], [110], and [111] [see Figs. 1(a)–1(c)], grown on STO substrate are calculated. The mismatch between material and substrate is: $\sim 1.9\%$ (LTO) and $\sim 3.4\%$ (CVO) for [001] superlattice; $\sim 1.7\%$ (LTO) and $\sim 3.5\%$ (CVO) for [110] superlattice; $\sim 1.8\%$ (LTO) and $\sim 3.4\%$ (CVO) for [111] superlattice. The possible magnetic ground states of superlattices are investigated firstly. For [001] and [110] cases, the local magnetic moments of Ti are nearly quenched to zero, and Ti's moment along the [111] direction is also significantly reduced compared to the bulk LTO ($\sim 0.68\ \mu_B$/Ti), as shown in Table 1, which suggests that the magnetic ground states of superlattices mainly depend on V ions. In our calculations, the two V ions in the minimal cell are coupled antiferromagnetically.

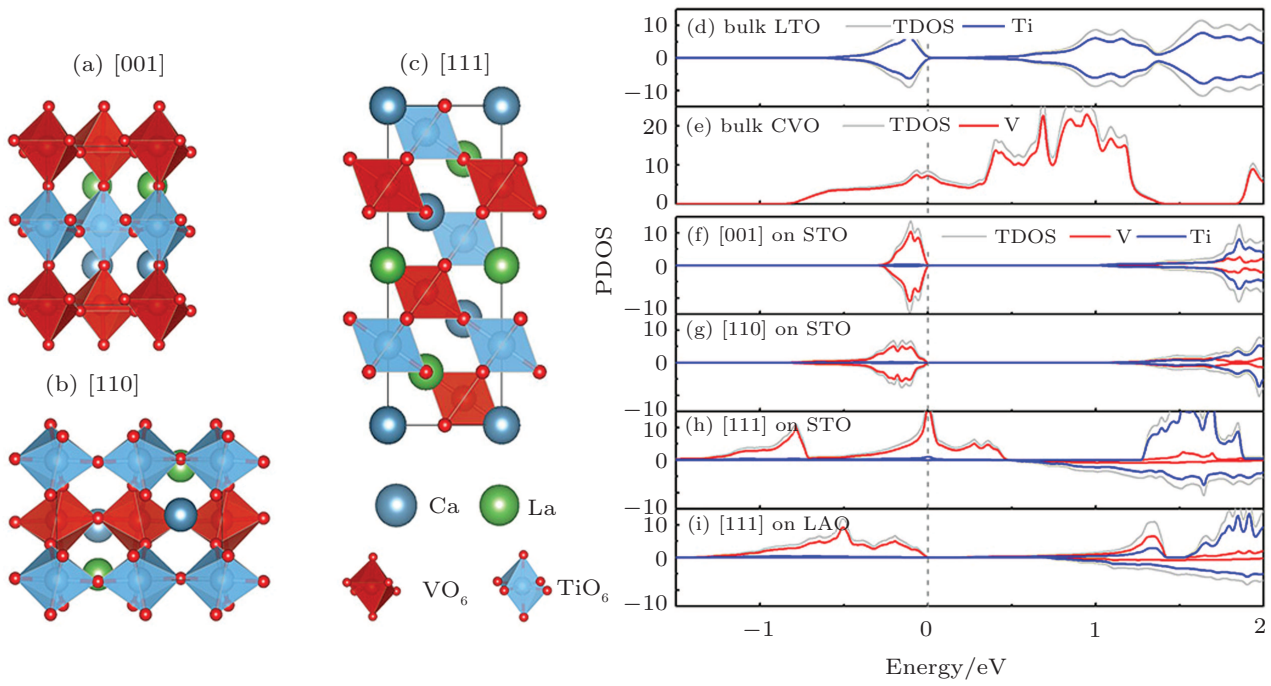


Fig. 1. (a)–(c) Sketch of $(LaTiO_3)_1/(CaVO_3)_1$ superlattices stacking along the [001], [110], and [111] directions, respectively. (d) and (e) PDOS for bulk $LaTiO_3$ and $CaVO_3$. (f)–(i) PDOS for $(LaTiO_3)_1/(CaVO_3)_1$ superlattices grown on $SrTiO_3$ substrate along the [001], [110], and [111] directions, respectively. (i) [111]-oriented superlattice grown on $LaAlO_3$ substrate. The Fermi level for each case is marked by a (black) broken line. The V and Ti atoms are represented by red and blue spheres, respectively.

Table 1. Summary of DFT results. The magnetic moments of ground state are calculated. The magnetic moment M_V (M_{Ti}) is in units of μ_B/V(Ti). The degree of charge transfer from Ti to V can be intuitively obtained from the corresponding magnetic moments.

$(LTO)_m/(CVO)_n$	Substrate	Orientation	M_V	M_{Ti}
$m=1,n=1$	STO	[001]	1.78	0.00
		[110]	1.79	0.00
		[111]	1.71	0.17
	LAO	[111]	1.74	0.10
$m=1,n=2$	STO	[001]	1.03 1.73	0.00
$m=2,n=2$	STO	[001]	1.74 1.74	0.00 0.00

Phenomenologically, considering the d^1 configuration of bulk LTO (Ti^{3+}) and CVO (V^{4+}), the local magnetic moments of both Ti and V ions should be close to 1 μ_B in theory. However, as shown in Table 1, the local magnetic moments of Ti ions are all significantly reduced to ~ 0 or ~ 0.17 μ_B/Ti for $(LTO)_1/(CVO)_1$ superlattices. Meanwhile, the corresponding V's moments are promoted to ~ 1.78, ~ 1.79, and ~ 1.71 μ_B/V for such three orientations respectively, indicating that the valence state of V ion in superlattices is not V^{4+}. Combined with the changes of magnetic moments between Ti ion and V ion, charge transfer from Ti^{3+} to V^{4+} should occur, which can be represented as: Ti^{3+} (d^1)/V^{4+} (d^1)-Ti^{4+} (d^0)/V^{3+} (d^2), similar to the charge transfer in $LaTiO_3/LaVO_3$ superlattices.[40] In addition, one can see that different orientations present different degrees of charge transfer [see Table 1]. For [111]-oriented case, the charge transfer is incomplete, *i.e.*, partial charge transfer, making electrons itinerant and thus rendering metallic behavior, as shown in Fig. 1(h). However, for [001] and [110] cases, the charge transfer from Ti to V becomes complete, leading to insulating behavior, as shown in Figs. 1(f) and 1(g). Therefore, orientation-dependent MIT is observed in $(LTO)_1/(CVO)_1$ superlattice.

In fact, such phenomena including charger transfer and orientation-dependent metal–insulator transition have been emphasized in $LaTiO_3/LaVO_3$ superlattices.[40] However, for $LaTiO_3/LaVO_3$ superlattices, the [001] case exhibits metallic behavior which is contrary to our calculations due to the different structural distortions between $LaVO_3$ and $CaVO_3$. Since A-site ion of $CaVO_3$ is smaller than that of $LaVO_3$, the bandwidth of 3d orbitals would be reduced by such a relatively strong $GdFeO_3$-type distortion of $CaVO_3$, which prefers the insulating behavior, as shown in Fig. 1(f). Following this argument, the strain effects closely related to the lattice distortion will be studied next.

3.2. Epitaxial strain

In general, the physical properties of perovskite oxides are very sensitive to the epitaxial strain,[41–45] and due to this sensitivity, structural distortions imposed by epitaxial strain can introduce strong changes in the electronic structures. Taking [111]-oriented superlattice as an example, LAO substrate with smaller lattice constants is adopted as stronger strain compared with STO substrate. As shown in Fig. 1(i), insulating behavior is presented when $LaAlO_3$ substrate is applied, as expected. Thus, besides stacking orientation, epitaxial strain is also an effective physical method to achieve MIT in this system. By comparing the magnetic moments with STO substrate, it is found that the Ti's magnetic moment of the superlattice on LAO substrate is reduced to ~ 0.1 μ_B and the corresponding V's moment is promoted to ~ 1.74 μ_B, as indicated in Table 1, suggesting enhanced charge transfer from Ti^{3+} to V^{4+}.

The underlying physical mechanism of such strain-induced MIT should be attributed to the lattice distortions. To confirm this argument, the Ti–O bond lengths and Ti–O–V bond angles are calculated, as demonstrated in Fig. 2, which show some obvious differences between LAO substrate and STO substrate. First, the Ti–O–V bond angles on STO substrate are straighter than that on LAO substrate, which facilitates the electron hopping and thus gives rise to a wider bandwidth [see Fig. 1(h)]. Second, the Ti–O bond lengths of the superlattice grown on STO substrate are almost equal, while LAO substrate shows a slight difference between these Ti–O bond lengths, as shown in Fig. 2. In addition, the Ti–O bond lengths on LAO substrate are smaller than that on STO substrate, indicating a shrunk size of oxygen octahedral cage, in agreement with higher valence of Ti that originated from the enhanced charge transfer from Ti to V.

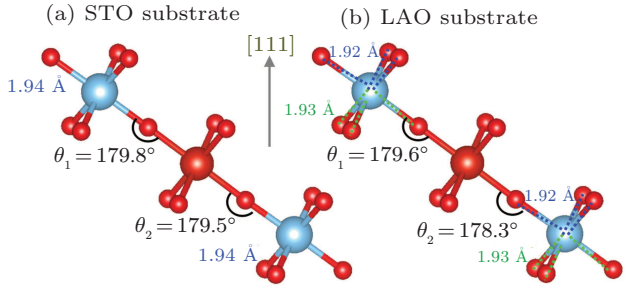


Fig. 2. The optimized Ti–O–V bond angles and Ti–O bonds lengths for [111]-oriented $(LaTiO_3)_1/(CaVO_3)_1$ superlattices grown on (a) $SrTiO_3$ substrate and (b) $LaAlO_3$ substrate. Ti, V, and O atoms are represented by blue, larger and smaller red spheres, respectively.

To reveal the evolution of electronic properties upon biaxial strains, the lattice constant a' of substrate within a wide range from 3.75 Å to 3.95 Å is scanned, as shown in Fig. 3.

When a' is greater than 3.90 Å, the system presents metallic behavior and the corresponding Ti's moment is about $\sim$ 0.17 μ_B, rendering a partial charge transfer from Ti to V. Such the incomplete charge transfer can be visualized by spatial distribution of the electron density of Ti ion. However, the charge transfer is enhanced when a' is less than 3.85 Å, leading to insulating behavior. Therefore, the metal–insulator transition in the [111]-oriented superlattice can be effectively tuned by the epitaxial strain.

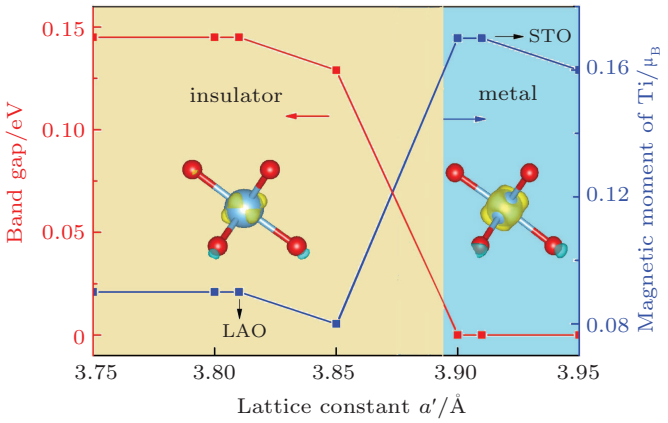


Fig. 3. The ground-state phase diagram of the [111]-oriented superlattice $(LaTiO_3)_1/(CaVO_3)_1$ as a function of biaxial strain. Insulating and metallic regions are distinguished by yellow and blue colors. The red line and blue line denote the band gap (left axis) and magnetic moment of Ti (right axis). The in-plane lattice constants of the superlattice are fixed to match the $a' \times \sqrt{2}$ Å. Here, the Ti's spatial distribution of the electron density corresponds to $a' = 3.80$ Å (left) and $a' = 3.90$ Å (right).

3.3. Thickness periods

Besides the structural orientation and strain effect, the thickness periods can also dramatically tune the physical properties of superlattices, such as the magnetic transition[46,47] and hybrid ferroelectricity.[38,40] In view of this, it is necessary to study the effect of thickness on LTO/CVO superlattices. Here, the [001]-orientated $(LTO)_1/(CVO)_2$ and $(LTO)_2/(CVO)_2$ superlattices grown on the STO substrate will be studied.

Before investigating the electronic structures of the superlattices $(LTO)_1/(CVO)_2$ and $(LTO)_2/(CVO)_2$, the ground magnetic states are studied. In these two cases, Ti's magnetic moments are all quenched due to the complete charge transfer, as shown in Table 1. Meanwhile, V's layers exhibit a C-AFM configuration (*i.e.*, antiferromagnetic coupling in-plane but ferromagnetic coupling along the c axis). For $(LTO)_1/(CVO)_2$ superlattice, the total density of states and the partial density of states are shown in Figs. 4(a)–4(c). The system is insulating with an obvious energy gap. Due to the complete charge transfer from Ti to V, the bands near the Fermi level are mostly contributed by V's 3d orbitals. Interestingly, considering the special structure of each LTO unit stacked two CVO units, there are two options for charge transfer from the Ti to V:

(i) The electron can be equally shared by the two V ions (*i.e.*, V ions have the formal valence of +3.5);

(ii) The electron can be localized in one of them (*i.e.*, V ions have mixed formal valences of +3 and +4).

In our calculations, the case of charge ordering has the lower energy than that without charge ordering. As indicated in Table 1, such two V's local moments are $\sim$ 1.03 μ_B and $\sim$ 1.73 μ_B respectively, suggesting an alternating V^{3+}/V^{4+} charge ordering. Such the selective charge transfer is because of the expansion of the V–O octahedra around the doped electrons, similar to the $(LaFeO_3)_2/(LaTiO_3)_1$ superlattice.[48,49] To confirm this argument, the V–O bond lengths are calculated. We found that the average V^{3+} bond length (2.01 Å) is larger than the average V^{4+} bond length (1.97 Å), suggesting the expansion of the octahedron, an energetically favorable distortion. As shown in Figs. 4(b) and 4(c), for the V ion in layer 1, the d_{xy} is occupied by one electron (*i.e.*, V^{4+}), while both d_{yz} and d_{xz} orbitals of V ion in layer 2 are fully occupied (*i.e.*, V^{3+}), which can be visualized by the spatial distribution of electrons [see Fig. 4(e)]. The electron disproportion of V ions between layer 1 and layer 2 is very clear. As shown in Fig. 4(e), the electron cloud surrounding V^{4+} ion (*i.e.*, V ion in layer 1) is d_{xy} shaped, while for the V^{3+} ion (*i.e.*, V ion in layer 2), the shape of electron cloud is formed by coupling d_{xz} and d_{yz} orbitals. Therefore, orbital ordering between layer 1 and layer 2 is also presented in $(LTO)_1/(CVO)_2$ superlattice.

For $(LTO)_2/(CVO)_2$ superlattice, the charge transfer still occurs and is also complete from Ti to V, as indicated in Table 1, similar to the $(LTO)_1/(CVO)_1$ and $(LTO)_1/(CVO)_2$ cases. However, the system has an obvious tendency to become metallic, as shown in Fig. 4(d). According to previous reports,[40,46] such weak metallicity, *i.e.*, small DOS values at Fermi level, can be enhanced by further increasing thickness. By comparing the electronic structures of these three [001] cases, one can see that the appearance of metal behavior is due to the shift of Ti's conduction band. Therefore, the Ti's physical environment is analyzed to understand such the thickness-dependent metal–insulator transition. For both $(LTO)_1/(CVO)_1$ and $(LTO)_1/(CVO)_2$ superlattices, each Ti has four in-plane nearest-neighbor Ti, while in $(LTO)_2/(CVO)_2$ superlattice, each Ti has five nearest-neighbor Ti, resulting in an expanded dimension, which will broaden the bandwidth. In addition, with increasing thickness, the reduced interface/volume ratio can also seriously affect the electronic structures. Thus, MIT in this system is tuned by these two factors.

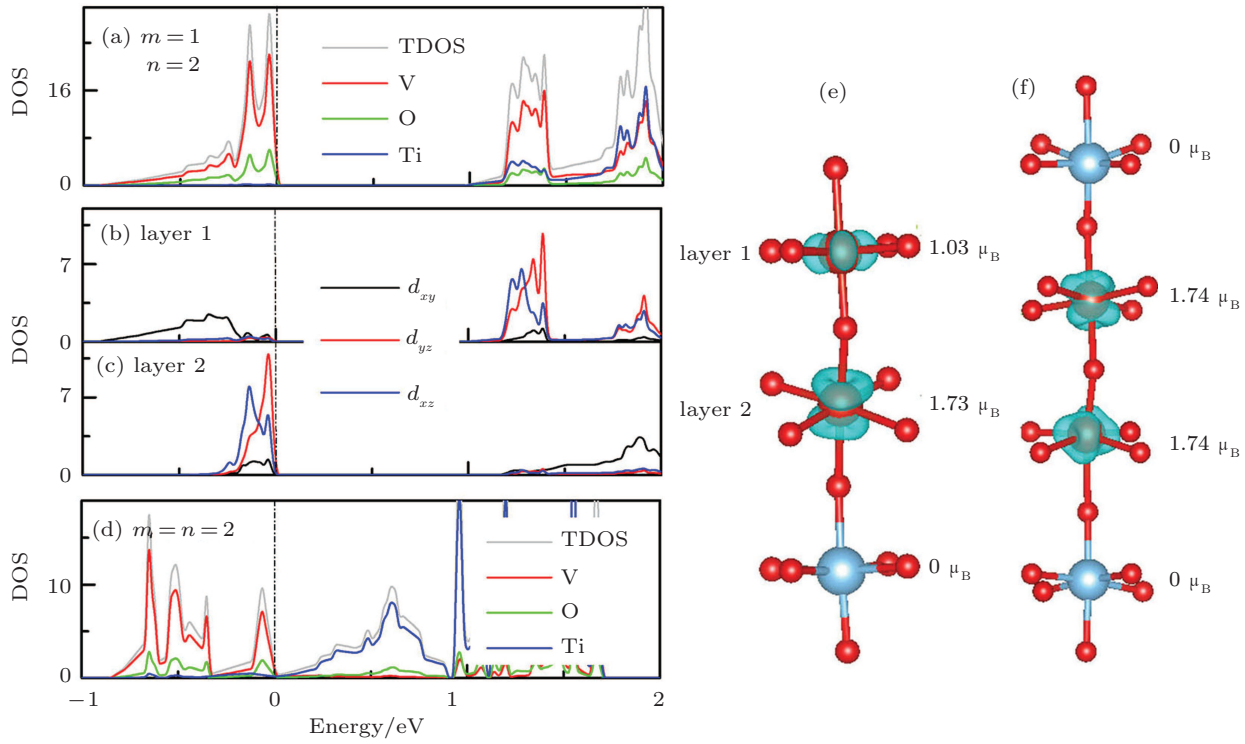


Fig. 4. (a) PDOS of [001]-oriented $(LaTiO_3)_1/(CaVO_3)_2$ superlattice and the corresponding orbital-resolved PDOS around the Fermi level for $CaVO_3$ bilayer: (b) layer 1, (c) layer 2. (d) DOS of [001]-oriented $(LaTiO_3)_2/(CaVO_3)_2$ superlattice. The black dotted line represents the Fermi level. The corresponding spatial distribution of the electron density and local magnetic moments for the cases of (e) $(LaTiO_3)_1/(CaVO_3)_2$ superlattice and (f) $(LaTiO_3)_2/(CaVO_3)_2$ superlattice. Ti, V, and O atoms are represented by blue, larger and smaller red spheres, respectively.

4. Conclusion

In summary, metal–insulator transition in the LTO/CVO superlattice has been studied using the first-principles calculation. It is found that metal–insulator transition in this system can be tuned by stacking orientation, epitaxial strain, and thickness periods. The $(LTO)_1/(CVO)_1$ superlattice on STO substrate shows insulating behavior when stacking along [001] and [110] orientations and metallic behavior when stacking along [111] orientation. For the [111]-oriented $(LTO)_1/(CVO)_1$ superlattice, metal–insulator transition is presented when STO substrate is replaced by LAO substrate. For the [001]-oriented $(LTO)_m/(CVO)_n$ superlattices on STO substrate, the highly probable metal–insulator transition appears by changing the thickness periods. Furthermore, many interesting topics, such as selective charge transfer, charge, and orbital ordering, are also presented in $(LTO)_1/(CVO)_2$ superlattice.

References

[1] Dagotto E 2005 *Science* **309** 257

[2] Dong S, Liu J M, Cheong S W and Ren Z 2015 *Adv. Phys.* **64** 519

[3] Dong S and Liu J M 2012 *Mod. Phys. Lett. B* **26** 1230004

[4] Picozzi S and Ederer C 2009 *J. Phys.: Condens. Matter* **21** 303201

[5] Imada M, Fujimori A and Tokura Y 1998 *Rev. Mod. Phys.* **70** 1039

[6] Kim B, Liu P, Tomczak J M and Franchini C 2018 *Phys. Rev. B* **98** 075130

[7] Golalikhani M, Lei Q, Chandrasena R, Kasaei L, Park H, Bai J, Orgiani P, Ciston J, Sterbinsky G, Arena D, Shafer P, Arenholz E, Davidson B, Millis A, Gray A and Xi X 2018 *Nat. Commun.* **9** 2206

[8] Paul A, Mukherjee A, Dasgupta I, Paramekanti A and Dasgupta T S 2019 *Phys. Rev. Lett.* **122** 016404

[9] Peil O E, Hampel A, Ederer C and Georges A 2019 *Phys. Rev. B* **99** 245127

[10] Shen M L, Weng Y K, Yi Y W, Geng Q F, Yan W, Wang H Y, Yang J P and Li X A 2019 *J. Appl. Phys.* **126** 085307

[11] Liu H D 2019 *Chin. Phys. B* **28** 107102

[12] Yang L J, Wu L Z and Dong S 2015 *Chin. Phys. B* **24** 127702

[13] Guo H W, Noh J, Dong S, Rack P, Gai Z, Xu X S, Dagotto E, Shen J and Ward T 2013 *Nano Lett.* **13** 3749

[14] Saleem M S, Song C, Peng J J, Cui B, Li F, Gu Y D and Panb F 2017 *Appl. Phys. Lett.* **110** 072406

[15] Beck S, Sclauzero G, Chopra U and Ederer C 2018 *Phys. Rev. B* **97** 075107

[16] Ruzmetov D, Gopalakrishnan G, Ko C, Narayanamurti V and Ramanathan S 2010 *J. Appl. Phys.* **107** 114516

[17] Scherwitzl R, Zubko P, Lezama I G, Ono S, Morpurgo A F, Catalan G and Triscone J M 2010 *Adv. Mater.* **22** 5517

[18] Zhang K H L, Du Y, Sushko P V, Bowden M E, Shutthanandan V, Sallis S, Piper L F J and Chambers S A 2015 *Phys. Rev. B* **91** 155129

[19] Lee J H and Rabe K M 2011 *Phys. Rev. Lett.* **107** 067601

[20] Dagotto E 2007 *Science* **318** 1076

[21] Mannhart J and Schlom D G 2010 *Science* **327** 1607

[22] Takagi H and Hwang H Y 2010 *Science* **327** 1601

[23] Hammerl G and Spaldin N 2011 *Science* **332** 922

[24] Bhattacharya A, May S J, Velthuis S G E te, Warusawithana M, Zhai X, Jiang B, Zuo J M, Fitzsimmons M R, Bader S D and Eckstein J N 2008 *Phys. Rev. Lett.* **100** 257203

[25] Dong S, Yu R, Yunoki S, Alvarez G, Liu J M and Dagotto E 2008 *Phys. Rev. B* **78** 201102

[26] Aruta C, Adamo C, Galdi A, Orgiani P, Bisogni V, Brookes N B, Cezar J C, Thakur P, Perroni C A, Filippis G D, Cataudella V, Schlom D G, Maritato L and Ghiringhelli G 2009 *Phys. Rev. B* **80** 140405

[27] Nanda B R K and Satpathy S 2009 *Phys. Rev. B* **79** 054428
[28] Ohtomo A and Hwang H Y 2004 *Nature* **427** 423
[29] Niu W, Chen Y D, Gan Y L, Zhang Y, Zhang X Q, Yuan X, Cao Z, Liu W Q, Xu Y B, Zhang R, Pryds N, Chen Y Z, Pu Y and Wang X F 2019 *Appl. Phys. Lett.* **115** 061601
[30] Cwik M, Lorenz T, Baier J, Muller R, Andre G, Bouree F, Lichtenberg F, Freimuth A, Schmitz R, Muller-Hartmann E and Braden M 2003 *Phys. Rev. B* **68** 060401
[31] Chamberland B L and Danielson P S 1971 *J. Solid State Chem.* **3** 243
[32] Komarek A C, Roth H, Cwik M, Stein W D, Baier J, Kriener M, Bourée F, Lorenz T and Braden M 2007 *Phys. Rev. B* **75** 224402
[33] Falcon H, Alonso J A, Casais M T, Martinez-Lope M J and Sanchez-Benitez J 2004 *J. Solid State Chem.* **177** 3099
[34] Perdew J P, Ruzsinszky A, Csonka G I, Vydrov O A, Scuseria G E, Constantin L A, Zhou X and Burke K 2008 *Phys. Rev. Lett.* **100** 136406
[35] Kresse G and Hafner J 1993 *Phys. Rev. B* **47** 558
[36] Kresse G and Furthmüller J 1996 *Phys. Rev. B* **54** 11169
[37] Dudarev S L, Botton G A, Savrasov S Y, Humphreys C J and Sutton A P 1998 *Phys. Rev. B* **57** 1505
[38] Zhang H M, Weng Y K, Yao X Y and Dong S 2015 *Phys. Rev. B* **91** 195145
[39] Park S Y, Kumar A and Rabe K M 2017 *Phys. Rev. Lett.* **118** 087602
[40] Weng Y K, Zhang J J, Gao B and Dong S 2017 *Phys. Rev. B* **95** 155117
[41] Dong S, Zhang Q F, Yunoki S, Liu J M and Dagotto E 2012 *Phys. Rev. B* **86** 205121
[42] Rondinelli J M and Spaldin N A 2011 *Adv. Mater.* **23** 3363
[43] Kumar D, David A, Fouchet A, Pautrat A, Varignon J, Jung C U, Lders U, Domengs B, Copie O, Ghosez P and Prellier W 2019 *Phys. Rev. B* **99** 224405
[44] Lu H S and Guo G Y 2019 *Phys. Rev. B* **99** 104405
[45] Weng Y K, Huang X, Tang Y K and Dong S 2014 *J. Appl. Phys.* **115** 17E108
[46] An M, Weng Y K, Zhang H M, Zhang J J, Zhang Y and Dong S 2017 *Phys. Rev. B* **96** 235112
[47] Wang X R, Li C J, Lü W M, Paudel T R, Leusink D P, Hoek M, Poccia N, Vailionis A, Venkatesan T, Coey J M D, Tsymbal E Y, Ariando and Hilgenkamp H 2015 *Science* **349** 716
[48] He X and Jin K J 2016 *Phys. Rev. B* **93** 161108
[49] Varignon J, Bibes M and Zunger A 2019 *Nat. Commun.* **10** 1658